

P5.7 A COMPARISON OF RAWINSONDE DATA FROM THE SOUTHEASTERN UNITED STATES DURING EL NIÑO, LA NIÑA, AND NEUTRAL WINTERS

Victoria Lynn Sankovich*
Pennsylvania State University, University Park, Pennsylvania

Joseph T. Schaefer and Jason J. Levit,
NOAA/NWS Storm Prediction Center, Norman, Oklahoma

1. INTRODUCTION

Meteorologists, as well as the public, have speculated on possible relations between the El Niño/ Southern Oscillation (ENSO) phases and severe weather events occurring in the United States. Schaefer and Tatom (1998) considered the number of tornadoes per year in the United States and sea surface temperatures (SST) in various portions of the Pacific Ocean to try to discern an impact of ENSO on the occurrence of tornadoes. Their statistical inquiries showed no major influence, but their data does show a signal that more tornadoes tend to occur in the mid-eastern states during the La Niña phase. Agee and Zurn-Birkhimer (1998) also use the annual total of United States tornadoes to attempt to determine a rise or decline in tornadoes during the El Niño phase. They conclude that tornado occurrences do not favor one ENSO phase but rather exhibit a shift in geographic location. For example, their results suggest that more tornadoes occur in the lower Midwest, Ohio Valley, Tennessee Valley, and mid-Atlantic region during the La Niña phase than in any other phase. Bove (1998), using the bootstrap method on tornado segments, found increased tornado activity over the Ohio and Tennessee River Valleys during the cold La Niña phase.

Marzban and Schaefer (2001) correlated various measures of tornado activity over various parts of the United States with the sea surface temperature in four different areas in the Pacific Ocean. The strongest correlation found was very small ($r = -0.07$), but there was a statistically significant, correlation between sea surface temperatures in the central tropical Pacific and the number of days with strong and violent tornadoes (F2 or greater on the Fujita Scale) in an area running from Illinois to the Atlantic Coast and Kentucky to Canada, i.e., a La Niña effect. Other correlations were smaller and generally not

statistically significant. An interesting paradox was noted by Browning (1998) in a study relating ENSO phase with severe thunderstorm activity in northwest Missouri. He found a tendency for fewer tornadoes during El Niño years and more tornadoes during La Niña years. In contrast, hail and wind storms showed the opposite tendency.

Because of the conflicting results from the various studies, it was decided to study meteorological conditions rather than historic weather events to try to get a clearer understanding of whether tornado and severe thunderstorm activity favors a specific ENSO phase. Kinematic and thermodynamic parameters calculated from rawinsonde data are examined in order to identify differences in the typical stratification of the atmosphere during the El Niño, La Niña, and Neutral ENSO phases. This study concentrates on the southeastern region of the United States (North Carolina, South Carolina, Georgia, Florida, Tennessee, Alabama, Mississippi, Arkansas, Louisiana, Oklahoma, and Texas) during the winter months (January, February, and March). These were chosen in agreement with Montroy (1997), who found that the months of November and January through March exhibit a connection between Pacific SST and precipitation in the southeastern region.

The Climate Prediction Center (CPC) has categorized every season by ENSO phase for all years dating back to 1950 by evaluating the SST of the area along the equator extending from 150 degrees west to the international dateline. The data are available from the CPC Internet site (Climate Prediction Center 2003a). The seasons classified as El Niño (EN) in this research are those categorized by the CPC as being either moderate EN or strong EN. La Niña (LN) was likewise classified. Weak EN and weak LN are grouped with the Neutral winters to create the Neutral (N) ENSO phase. Table 1 presents each winter with its corresponding ENSO phase.

This paper is divided into two sections. The first section focuses on parameters calculated from winter soundings associated with significant severe convective events from 1958 through 1996.

* Corresponding author: Victoria Lynn Sankovich,
3106 Algonquin Trail, Lower Burrell, PA 15068;
e-mail: vls148@psu.edu

In the second section, all 00 UTC soundings released from sites in the Southeastern United States during the winter months of 1958 through 2003 are considered. In both sections, the years are stratified by ENSO phase, and the characteristics of each grouping are examined and compared to see if the typical atmospheric structure during any specific ENSO phase is more compatible with severe thunderstorm occurrence.

2. METHODOLOGY

The following parameters are examined for each sounding: Lifted Index, Mixed Layer CAPE, Convective Inhibition, Surface–1 km Storm-Relative Helicity, Surface–3 km Storm-Relative Helicity, and Surface–6 km Bulk Shear. Also, two composite indices, the Supercell Composite Parameter and the Significant Tornado Parameter, are computed. Table 2 lists these parameters along with their relation to severe weather. These parameters are commonly used in forecasting severe weather and, when used together, give a general overview of the configuration of the atmosphere.

El Niño	Neutral			La Niña
1958	1957	1972	1988	1971
1966	1959	1975	1990	1974
1969	1960	1977	1991	1976
1973	1961	1978	1993	1989
1983	1962	1979	1994	1999
1987	1963	1980	1996	2000
1992	1964	1981	1997	
1995	1965	1982	2001	
1998	1967	1984	2002	
	1968	1985	2003	
	1970	1986		

Table 1: Winters classified by ENSO phase (1957–2003)

The parameters are categorized by ENSO phase (EN, N, and LN) and their distributions are calculated to determine if there is a higher or lower propensity for severe weather during the ENSO phases. Parameter distributions are analyzed via a box plot created with PSI Plot Version 6 software (Poly Software International 1999). The box plot

PARAMETER	DESCRIPTION	UNITS	CHARACTERISTIC FAVORING STORM DEVELOPMENT
Thermodynamic:			
Lifted Index (LI)	100-hPa Mean Layer Lifted Index at 300 hPa	°C	More Negative ML LI indicates more instability
CAPE	100-hPa Mean Layer CAPE	J kg ⁻¹	High CAPE
Convective Inhibition (CIN)	100-hPa Mean Layer Convective Inhibition	J kg ⁻¹	Higher CIN tends to prevent lifted parcels from reaching LFC, thus serving to limit deep convection
Kinematic:			
Bulk Shear (BKSHR) (magnitude of shear vector)	Surface–6 km Bulk Shear	knots	High SHR
1 km Storm-Relative Helicity (Sfc–1 km SRH)	SFC–1 km Storm-Relative Helicity	m ² s ⁻²	High Sfc–1 km SRH promotes rotation
3 km Storm-Relative Helicity (Sfc–3 km SRH)	SFC–3 km Storm-Relative Helicity	m ² s ⁻²	High Sfc–3 km SRH promotes rotation
Composite:			
Supercell Composite Parameter (SCP)	Combination of CAPE, SRH, Bulk Richardson Number	---	Supercells likely when SCP > 1
Significant Tornado Parameter (STP)	Combination of CAPE, SRH, BKSHR, and lifted condensation level	---	Significant Tornadoes likely when STP > 1

Table 2. Parameters analyzed from soundings

displays the minimum value, 10th percentile, 25th percentile, mean (50th percentile), 75th percentile, 90th percentile, and maximum values of the distribution. Using Fig. 1A as an example, the maximum and minimum values appear at the ends of the outer whiskers on the plot. The lower trapezoidal area of the shaded region represents the 10–25% portion of the data, and the upper trapezoidal shaded region is the 75–90% distribution. The central rectangle displays the inner 50% of the data, and the middle horizontal line is the mean.

2.1 Thermodynamic Parameters

The Lifted Index (LI) examined is the “100-hPa Mean Layer Lifted Index at 300 hPa.” It is the difference between the observed 300-hPa temperature and the temperature that the lowest 100-hPa mean parcel would have after being lifted to 300 hPa. It is similar to Galway’s Lifted Index (Galway 1956) except 300 hPa is used as the reference level instead of 500 hPa. By using 300 hPa, the index considers the lifted parcel buoyancy in the upper-troposphere.

Mean Layer Convective Available Potential Energy (CAPE) is the maximum amount of energy available to an ascending mean parcel from the lowest 100 hPa of the atmosphere. CAPE is computed using parcel theory and is the area on a thermodynamic diagram between the lifted parcel curve and the observed sounding. The more energy a lifted parcel has available, the greater the possibility of the atmosphere to evolve into a severe storm or tornado.

Convective Inhibition (CIN) is the amount of energy that a surface air parcel must gain in order to be lifted from its original height to its level of free convection (LFC) (Glickman 2000). The higher the CIN value, the more unlikely air is to reach its LFC and evolve into a severe convective storm. Therefore, this measurement is valuable in determining the probability of severe weather.

2.2 Kinematic Parameters

Surface–6 km Bulk Shear (BKSHR) is the magnitude of the shear vector between the winds at the surface and those at 6 km above ground level. This vector indicates the change of wind direction and speed across the lower troposphere. Severe weather is normally associated with high BKSHR, and as the severity of deep convection increases, BKSHR will also increase (Craven et al. 2002).

Storm-Relative Helicity (SRH) measures how rapidly storm inflow is bringing rotation into the storm. Mathematically, it is the inner product of the storm-relative winds and the streamwise vorticity. This parameter is generally related to the tendency for a supercell to rotate (Glickman 2000). The 1 km Storm-Relative Helicity (Sfc–1 km SRH) is the integral of SRH over the layer stretching from the surface to 1 km, and the 3 km Storm-Relative Helicity (Sfc–3 km SRH) is the integral over the lowest 3 km of the atmosphere.

2.3 Composite Parameters

The two composite parameters considered were first presented in Thompson et al. (2003). They provide a preliminary screen of rawinsonde data to identify environments most capable of supporting severe convection.

The Supercell Composite Parameter (SCP) is a combination of the CAPE of the most unstable parcel in the lowest 300 mb (MUCAPE), the Sfc–3 km SRH, and the square of the difference between the density weighted winds in the Surface to 6 km layer and those in the Surface to 500 m layer (this wind is often called the Bulk Richardson Number or BRN shear). SCP can be computed from the formula:

$$\text{SCP} = (\text{MUCAPE}/1000 \text{ J kg}^{-1}) \\ \bullet (\text{Sfc-3 km SRH}/100 \text{ m}^2\text{s}^{-2}) \\ \bullet (\text{BRN shear}/40 \text{ m}^2\text{s}^{-2}).$$

A study of RUC–2 soundings found that values of SCP greater than 1 generally favor supercell storms.

The Significant Tornado Parameter (STP) is similar to SCP. The STP aims to discriminate between environments compatible with significant tornadic activity and those compatible with non-tornadic supercell storms. The formula for STP is:

$$\text{STP} = (\text{CAPE}/1000 \text{ J kg}^{-1}) \\ \bullet (\text{BKSHR}/39 \text{ kt}) \\ \bullet (\text{Sfc-1 km SRH}/100 \text{ m}^2\text{s}^{-2}) \\ \bullet ([2000 - \text{LCL height}]/1500 \text{ m}).$$

An STP value of 1 appears to be a reasonable criteria to discriminate between non-tornadic supercells and significant tornado environments.

It must be emphasized that SCP and STP do not uniquely indicate severe weather potential. They simply provide a first-guess discrimination of areas where storm potential will exist.

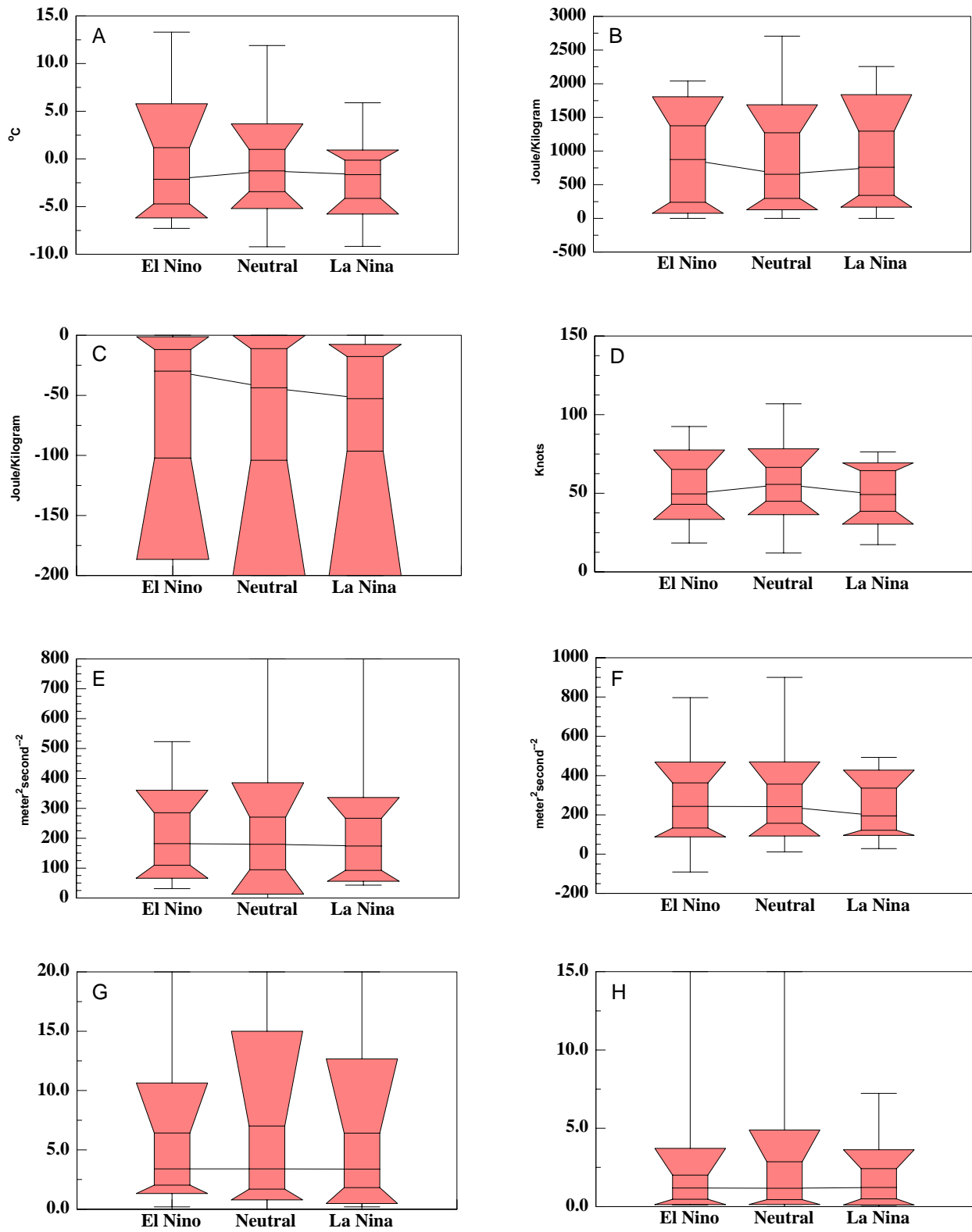


FIGURE 1: Box plots for parameters associated with severe weather soundings: A) Lifted Index; B) Mixed Layer CAPE; C) Convective Inhibition; D) Surface-6 km Bulk Shear; E) Surface-1 km Storm-Relative Helicity; F) Surface-3 km Storm-Relative Helicity; G) Supercell Composite Parameter; H) Significant Tornado Parameter

3. SEVERE WEATHER SOUNDINGS

Atmospheric conditions associated with severe thunderstorms are examined to see whether the ENSO phase affects the atmospheric structure associated with severe thunderstorm activity.

3.1 Data

An expanded version of the significant severe thunderstorm proximity dataset created by Brooks and Craven is utilized (Brooks and Craven 2002; Craven et al. 2002; Craven and Brooks 2004). It consists of parameters computed from rawinsondes that were released within 100 nautical miles (185.3 km) and 3 hours of significant wind events (gusts greater than or equal to 65 knots), significant hail occurrences (hail greater than or equal to 2"), and/or significant tornadoes (tornadoes rated F2–F5) during the period 1957 through 1996, inclusive. (The original Brooks and Craven database only considered the period 1997–1999.) Of the 3,243 proximity soundings, 266 were taken during the winter months (January, February, March). Since the data sample is so small and over 90% of the soundings were taken in the Southeast, the entire winter proximity dataset is examined. These data were then sorted by ENSO Phase (Table 3). Over two-thirds (67.3%) of the proximity soundings were collected during Neutral (N) years, 17.3% in La Niña (LN) years, and 15.4% in El Niño (EN) years. This compares to 70% of the years being Neutral, 20% La Niña, and 10% El Niño.

ENSO Phase	Number of Proximity Soundings	Number of years
El Niño	41	8
Neutral	179	28
La Niña	46	4

Table 3: Proximity Soundings by ENSO Phase

3.2 Analysis

The 300-hPa LI box charts (Fig. 1A) indicate very little difference in the lower 75% of the datasets associated with each ENSO phase. The median values are (-2.1, -1.2, -1.6) for (EN, N, LN), and the 10% values are (-6.1, -5.1, -5.6) respectively. When it is noted that rawinsonde temperature accuracy is only about $\pm 0.3^\circ\text{C}$ (Elliott and Gaffen 1991), these values are virtually the same. However, there are differences apparent on the stable (positive) side of the LI distributions,

with the 90th percentile values being (5.8, 3.7, 1.3). It is quite likely that the proximity soundings that show marked stability are not representative of the actual severe thunderstorm environment since Brooks and Craven did not consider the synoptic situation associated with individual soundings. Many of these soundings may have sampled the cold side of a frontal system while the storms occurred in the warm sector.

The mixed layer CAPE (Fig. 1B) analysis supports this interpretation. All the proximity soundings indicate unstable conditions with CAPE of zero J kg^{-1} or higher (Fig. 1B), and only three of the soundings had zero J kg^{-1} CAPE. Since CAPE is a vertically integrated parameter, this adds credence to the speculation that the soundings with positive LIs are not representative of the actual storm environment. There is very little difference in the CAPE distributions between the three ENSO phases.

In order to show resolution in the CIN distributions, it was necessary to limit the minimum value displayed. All CINs lower than -200 J kg^{-1} were arbitrarily set to -200 J kg^{-1} for the analysis. (While this caused a slight change in the 10th percentile level for both the N and LN groups, it did not change any of the other plotted thresholds.) Also, since the upper limit of CIN is zero by definition, values computed to be greater than zero must arrive from erroneous input data and are ignored. The relatively high median value of CIN (Fig. 1C) for EN storms is again probably caused by the unrepresentative data in several of the soundings.

The Surface–6 km BKSHR for severe weather is shown in Fig. 1D. At first glance it appears as though the distributions are somewhat different because the LN phase has a very tight 75–90% spread compared to the EN and N phases. However, upon comparison of the middle 50% spread of the data, it is apparent that each phase is actually quite similar to the others: 43–67 kt is the EN 50% spread, 39–64 kt is the LN 50% spread, and 45–67 kt is the N 50% spread. Hence, BKSHR associated with severe convection is relatively independent of ENSO phase.

Because of extreme outliers, the Surface–1 km SRH data is arbitrarily capped at $800 \text{ m}^2\text{s}^{-2}$. Similarly, since positive values of SRH are most compatible with the occurrence of cyclonic storms, zero is used as a lower limit. This expediently removes erroneous data, albeit at the expense of a few negative outliers. In general, the spread of the Sfc–1 km SRH data for the three different ENSO phases (Fig. 1E) is very similar, except that the N group has a greater spread between the 10th

percentile and 90th percentile values. When the depth of the integration is increased to Surface–3 km (Fig. 1F), the SRH had fewer extreme values so the distributions can be displayed without truncation. Neither helicity value gives an indication of having a dependence on its associated ENSO phase.

Since supercell composite parameter (SCP) values greater than 1 suggest conditions that strongly favor supercells, positive outliers are capped at 20. (Note that all of these very high values lie above the 90th percentile level.) Additionally, since conditions that would make SCP less than zero are not conducive to storm development, negative values are truncated from the distribution as potentially non-representative of the near storm environment. For the winter proximity dataset, there was only one negative reading (computed from a Neutral ENSO sounding). Although the spread between the middle 50% of the distribution is wider for the Neutral distribution than the other two ENSO phases (Fig. 1G), the three phases for SCP (Fig. 1G) are quite similar. The median values are (3.46, 3.4, and 3.09) for (EN, N, LN).

Similar reasoning leads to capping the significant tornado parameter (STP) at 15. Again, this change only affects outliers beyond the 90th percentile level. The distribution is also truncated at zero in an attempt to eliminate non-representative values. The resulting box chart (Fig. 1H) is similar to that of the SCP. The median values are virtually the same, with the only apparent difference being that the width of the middle 50% for the Neutral phase is larger.

3.3 Interpretation

The eight parameters analyzed for winter severe thunderstorms in the United States suggest that severe weather is independent of ENSO phase. Severe thunderstorms develop from similar atmospheric stratifications regardless of the physical processes responsible for creating the pre-storm environment. Essentially, this is what allows us to make operational severe thunderstorm forecasts.

4. WINTER SOUNDINGS FROM THE SOUTHEASTERN UNITED STATES

The same sounding parameters that were used to evaluate the severe thunderstorm proximity soundings are computed for every 00 UTC rawinsonde release during the winter over a span of 46 years to see whether ENSO has a

consistent effect on the atmospheric structure that makes one phase more conducive to severe thunderstorm activity than others.

4.1 Data

The Storm Prediction Center (SPC) maintains an archive of sounding data collected from 1958 through the present. For this study, soundings taken in the Southeastern United States during the winter months at 00 UTC between 1958 and 2003, inclusive, are examined. Altogether, approximately 67,000 soundings are examined and categorized by ENSO phase. From these data, the same eight sounding parameters (three thermodynamic, three kinematic, and two composite) were examined because of their association with severe weather and severe thunderstorm development (Table 2).

4.2 Analysis

As would be expected from a study of all winter soundings, the typical atmospheric structure is extremely stable. The 300-hPa LI box charts (Fig. 2A) indicate very little difference in the upper 75% of the data categories. The median LIs are (14.2, 14.8, 12.0) for (EN, N, LN) respectively. However, the 10th percentile values are (2, 1.25, -0.5) respectively. This indicates that there are more unstable LIs associated with La Niña years than with Neutral or El Niño ones. It must be noted that the extreme values of negative LI observed during all three ENSO phases (-10.3, -12.6, -11.0) are comparable.

Since the vast majority of soundings are stable (ML Cape is less than or equal to zero J kg^{-1} on 74.6% of the soundings), only cases where positive CAPEs exist were considered (Fig. 2B). For the unstable cases, the 75th and 90th percentile thresholds are higher during La Niña years, again indicating a tendency for more unstable days during the cold ENSO phase.

To allow for resolution in the box plots, CIN values are capped at -200 J kg^{-1} . This only impacts the data that is less than the lowest 10% of any of the distributions (Fig. 2C). In contrast to the LI and CAPE distributions, the 75th and 90th percentile thresholds indicate slightly less of a tendency during La Niña for CIN to prevent parcels to reach the LFC.

The Surface–6 km Bulk Shear data (Fig. 2D) contains some very extreme positive values. Because of this, the values were capped at 150 kt.

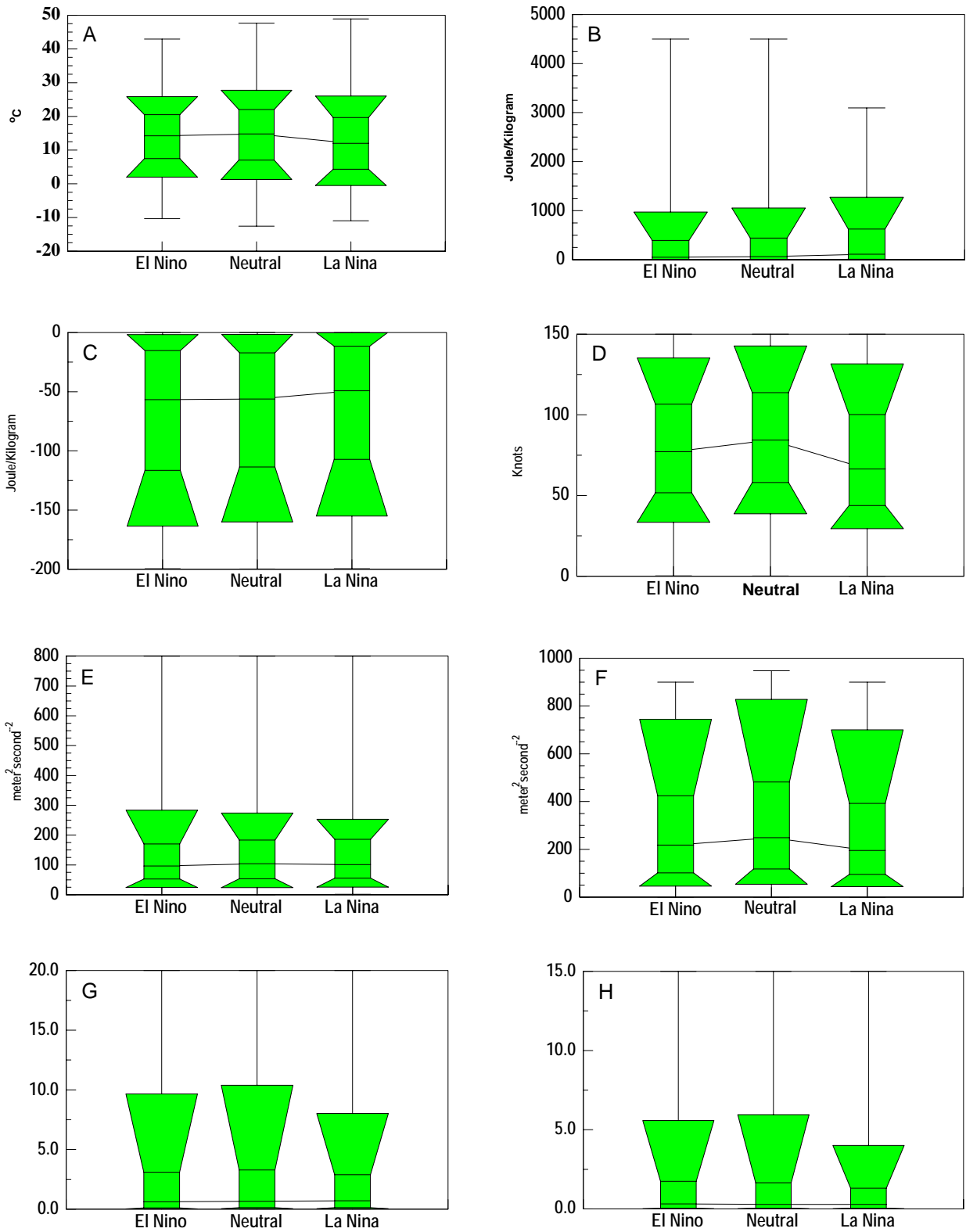


FIGURE 2: Box plots for parameters associated with all winter 00 UTC soundings from the Southeastern United States: A) Lifted Index; B) Mixed Layer CAPE; C) Convective Inhibition; D) Surface-6 km Bulk Shear; E) Surface-1 km Storm-Relative Helicity; F) Surface-3 km Storm-Relative Helicity; G) Supercell Composite Parameter; H) Significant Tornado Parameter

This only impacted the outliers; it had no effect on any of the thresholds plotted on the box chart. Since BKSHR is the magnitude of the vector difference and by definition must be a positive number, values less than zero indicated erroneous input data. There is slightly higher BKSHR during the N and EN phases than during the LN phase. This is apparent in the median values of (77, 84, 66) for (EN, N, LN). The 25% value for LN is approximately equal to the 10% values of both the EN and N phases. This again suggests weaker shear during LN.

To expeditiously remove outliers and erroneous data, Surface–1 km Storm-Relative Helicity is again capped at $800 \text{ m}^2\text{s}^{-2}$, and values less than zero were truncated from the data distributions. The Surface–1 km SRH graph shows very little dependence on ENSO phase (Fig. 2E).

The situation changes when a deeper layer is used in the computation of the SRH. The Surface–3 km SRH distributions (Fig. 2F) display an ENSO dependence similar to that shown by the Surface–6 km Bulk Shear. There is somewhat less Surface–3 km SRH present in the wintertime atmosphere over the Southeastern United States during La Niña than during the other phases. Further, the Neutral phase typically has a stratification that results in more Surface–3 km SRH than the other phases.

To display the supercell composite parameter distributions, the series have been truncated at zero since generally only positive values are compatible with supercell development. Further, positive outliers are capped at 20, which does not change any of the thresholds shown in the box chart (Fig. 2G). The lowest 75% of the positive STP values has virtually the same distribution regardless of the ENSO phase. The 75th percentile values are (3.1, 3.3, 2.9) for (EN, N, LN). However, the 90th percentile values are (9.7, 8.0, 10.4).

Using similar reasoning as stated with the supercell composite parameter, the significant tornado parameter (Fig. 2H) was truncated at zero, and the capping maximum value was set at 15. The STP distributions are very similar to those of the SCP: the lowest 75% of the positive values for all three ENSO phases has virtually the same distribution. However, there are marked differences in the 90th percentile values of (5.6, 6.0, 4.0).

4.3 Results

The thermodynamic and kinematic parameters have produced contrasting results concerning which, if any, ENSO phase is more apt to produce severe weather. The thermodynamic parameters (LI, CAPE, CIN) reveal that the structure of the atmosphere is slightly more favorable for severe weather (unstable) during the La Niña phase. In contrast, the kinematic parameters (BKSHR, Surface–1 km SRH, Surface–3 km SRH) are more favorable for severe weather during the EN and N phases. [The composite parameters (SCP, STP), which are a combination of both thermodynamic and kinematic parameters, indicate a slightly higher propensity for supercell and significant tornado development over the southeastern United States during the winter in Neutral and El Niño years than in the La Niña phase years.]

5. DISCUSSION AND CONCLUSIONS

Analysis of significant severe thunderstorm proximity sounding data indicates that severe storms develop under the same conditions regardless of ENSO phase. Thus, as long as appropriate synoptic conditions arise, severe weather will occur. The question then remains: do parameters related with severe thunderstorms occur more frequently during any ENSO phase?

All 00 UTC soundings taken over the southeastern United States during the winter months of 46 years were examined in an attempt to determine if favorable conditions for storms are preferentially found during any ENSO phase. Mixed signals are revealed. The thermodynamic parameters favor storm development during the LN phase, and the kinematic parameters favor storm development during the EN and N phases. When empirical composite parameters are considered, it is seen that there is a slight preference for winter severe thunderstorm activity in the southeast to be suppressed during La Niña years.

These findings are physically reasonable when the typical jet stream patterns associated with the three ENSO phases are considered (Climate Prediction Center 2003b). During the warm EN phase, the jet stream generally enters the United States through the southwestern states below the Rocky Mountain plateau so that the jet is typically positioned above the Gulf Coast over the southeast. This promotes relatively strong winds in the mid- to upper-troposphere and thus produces high values of the kinematic parameters.

Northwest of the jet stream, relatively cool, dry conditions prevail.

The cool LN phase is in contrast to the EN phase. The jet stream enters the western United States through the northwestern states (above the Rocky Mountains). The resulting lee trough over the eastern United States typically positions the jet stream across the southeastern states farther to the north. This lowers the values of the kinematic parameters, but the vertical circulations associated with the jet bring warm, moist low-level air into the area south of the jet and increase the magnitude of the thermodynamic sounding parameters over the area.

It must be emphasized that these differences are subtle. Like all climatological signals, they represent long-term trends. They do not provide a tool for making seasonal or other extended forecasts; rather, they show that other things being equal, the atmospheric stratification over the Southeastern United States is typically less compatible for the occurrence of severe thunderstorms (3/4" or larger hail, thunderstorm gusts of 58 mph or faster, tornados) during a La Niña winter than during Neutral or El Niño winters.

Acknowledgements: This paper grew out of an Oak Ridge Institute for Science and Education (ORISE) summer intern program project by the lead author (VS) at the Storm Prediction Center. This program was funded by NOAA's National Weather Service EEO Office. The University of Oklahoma and the National Severe Storms Laboratory assisted with the actual arrangements for the program. Richard Naden, Peggy Stogsdill, Linda Crank, and Daphne Zaras deserve special recognition.

6. REFERENCES

- Agee, E., and S. Zurn-Birkhimer, 1998: Variations in USA tornado occurrences during El Niño and La Niña. Preprints, *19th Conf. on Severe Local Storms*, Minneapolis, MN, Amer. Meteor. Soc., 287-290.
- Bove, M.C., 1998: Impacts of ENSO on United States tornadic activity. Preprints, *19th Conf. on Severe Local Storms*, Minneapolis, MN, Amer. Meteor. Soc., 313-316.
- Brooks, H. E., and J. P. Craven, 2002: A database of proximity soundings for significant severe thunderstorms. Preprints, *21st Conf. on Severe Local Storms*, San Antonio, TX, Amer. Meteor. Soc., 639-642.
- Browning, P., 1998: ENSO-related severe thunderstorm climatology of northwest Missouri. Preprints, *19th Conf. on Severe Local Storms*, Minneapolis, MN, Amer. Meteor. Soc., 291-292.
- Climate Prediction Center, 2003a: Cold and warm episodes by season. [Available online at http://www.cpc.ncep.noaa.gov/products/analysis_monitoring/ensostuff/ensoyears.html.]
- Climate Prediction Center, 2003b: El Niño and La Niña-related winter features over North America. [Available online at http://www.cpc.noaa.gov/products/analysis_monitoring/ensocycle/nawinter.html.]
- Craven, J. P., and H. E. Brooks, 2004: Baseline climatology of sounding derived parameters associated with deep, moist convection. *National Weather Digest*, in press.
- _____, _____, and J. A. Hart, 2002: A baseline climatology of soundings derived parameters associated with deep, moist convection. Preprints, *21st Conf. on Severe Local Storms*, San Antonio, TX, Amer. Meteor. Soc., 643-646.
- _____, R. E. Jewell, and H. E. Brooks, 2002: Comparison between observed convective cloud-base heights and lifting condensation level for two different lifted parcels. *Wea. Forecasting*, **17**, 885-890.
- Elliott, W. P., and D. J. Gaffen, 1991: On the utility of radiosonde humidity archives for climate studies. *Bull. Amer. Meteor. Soc.*, **72**, 1507-1520.
- Galway, J. G., 1956: The lifted index as a predictor of latent instability. *Bull. Amer. Meteor. Soc.*, **37**, 528-529.
- Glickman, T. S., Ed., 2000: *Glossary of Meteorology*. 2nd ed. Amer. Meteor. Soc., 855pp.
- Marzban, C. and J. T. Schaefer, 2001: The correlation between U.S. tornadoes and Pacific sea surface temperatures. *Mon. Wea. Rev.*, **129**, 884-895.

Montroy, D. L., 1997: Linear relation of central and eastern North American precipitation to tropical Pacific sea surface temperature anomalies. *J. Climate*, **10**, 541-558.

Poly Software International, 1999: *PSI-Plot Version 6, 8th Edition*, Poly Software International, Perl River, NY, 345 pp.

Schaefer, J. T., and F. B. Tatom, 1998: The relationship between El Niño, La Niña, and United States tornadoes. Preprints, *19th Conf. on Severe Local Storms*, Minneapolis, MN, Amer. Meteor. Soc., 416-419.

Thompson, R. L., R. Edwards, J. A. Hart, K. L. Elmore, and P. Markowski, 2003: Close proximity soundings within supercell environments obtained from the Rapid Update Cycle. *Wea. Forecasting*, **18**, 1243-1261.